EEET ECOLOGICAL ENGINEERING & ENVIRONMENTAL TECHNOLOGY

Ecological Engineering & Environmental Technology 2024, 25(7), 322–342
https://doi.org/10.12912/27197050/188282
ISSN 2719-7050, License CC-BY 4.0

Received: 2024.04.25
Accepted: 2024.05.22
Published: 2024.06.01

Techno-Economic and Environmental Analysis of a Renewable Hybrid System in Southern Morocco

Elmostafa Achbab[1,2*], Rachid Lambarki[2], Hassan Rhinane[2], Dennoun Saifaoui[1]

[1] Renewable Energy and System Dynamics Laboratory, Faculty of Sciences-Ain Chock, Hassan II University, Casablanca, Morocco

[2] Geosciences Laboratory, Faculty of Sciences-Ain Chock, Hassan II University, Casablanca, Morocco.

* Corresponding author's e-mail: mo.achbab@gmail.com

ABSTRACT

This article presents an assessment of the technical and economic feasibility of a 20 MW grid-connected wind-solar-photovoltaic hybrid system in the city of Dakhla, located in southern Morocco. During this study, GIS and virtual reality were integrated to model and simulate the productivity of the hybrid system under local climatic conditions. Additionally, 3D modeling of the system provides an immersive view to visually assess the system's impact on the local landscape and anticipate potential logistical challenges. By taking advantage of this technology, our study goes beyond traditional models, proposing an innovative approach to better understand the spatial and visual dimensions of the project. The results of our study, based on these state-of-the-art methodologies, reveal promising conclusions regarding its annual energy production, which is approximately 60 GW, the levelized cost of energy of the system, which is approximately LCOE = $0.045/kWh, the net present value (NPV) of $27,439,559.00, the internal rate of return (IRR) of 17.5%, and a discounted payback period (DPP) of 8 years. Additionally, from an environmental perspective, the hybrid system has the capacity to avoid approximately 936,494 tons of greenhouse gas emissions, equivalent to savings of approximately $18,729,875.00 in terms of carbon dioxide reduction over its lifetime.

Keywords: hybrid system, technical feasibility, GIS, virtual reality, economic analysis, environmental impact, renewable energy.

INTRODUCTION

As the world's pursuit of sustainable energy sources gains momentum, the integration of hybrid systems that harmonize wind and solar photovoltaic (PV) technologies emerges as a formidable solution to address energy demands while mitigating environmental impact. This integration not only capitalizes on the individual strengths of these resources but also holds promise for bolstering energy production, reliability, and system stability. In light of these considerations, the focus of this article is to conduct a comprehensive techno-economic analysis of a 20 MW hybrid wind-solar PV system, with particular emphasis on its suitability for grid integration. The selection of Dakhla City, Morocco, for this case study is driven by a confluence of factors that underscore its significance. The city is underpinned by its exceptional wind and solar resource potential, which is characteristic of the region. This bountiful availability resources forms the foundation of our investigation, offering an ideal setting to assess the technical and economic feasibility of a hybrid system. Moreover, the low population density in Dakhla City provides a distinct advantage, minimizing potential land-use conflicts and facilitating the large-scale implementation of wind and solar technologies. These local dynamics make Dakhla City an optimal testing ground for the integration of wind and solar PV resources, ultimately contributing to our understanding of renewable energy transitions. In addition, this study investigates the complex interplay between

technology, economics and environmental sustainability in the context of a hybrid system. By exploring the optimal fusion of wind and solar photovoltaic resources, our aim is not only to determine the economic viability of such a system, but also to elucidate its wider implications for the energy landscape of the city of Dakhla and its potential applicability in similar regions. Our detailed techno-economic assessment is based on a comprehensive understanding of the energy production, costs, revenues and environmental benefits arising from this transition. In addition, the study rigorously examines the resilience of the system to fluctuations in critical variables, thereby addressing the challenges of uncertainty and providing insight into its robustness.

REVIEW OF RELATED LITERATURE

The technical, economic, and environmental perspectives aspects of hybrid wind-solar PV systems constitute a crucial component in evaluating their feasibility and effectiveness as renewable energy solutions. In the Moroccan context, a recent study conducted by El-Houari et al. (2021) an in-depth energy, economic and environmental analysis was undertaken for an autonomous hybrid renewable energy system (HRES), combining wind and solar photovoltaic systems. The study employed HOMER Pro software to carry out economic evaluations and feasibility optimizations. To ensure a comprehensive assessment, simulations were conducted across 24 carefully chosen cities representing various climatic regions. Meteorological data for these cities was meticulously generated utilizing the NASA platform. For the study, a typical village in the Fez-Meknes region with a daily energy load of 319.35 kWh and a peak power demand of 30.89 kW served as the baseline. The evaluated LCOE exhibited a range between 0.32 $/kWh and 0.171 $/kWh. In this study, the city of Dakhla emerged with the lowest LCOE and demonstrated a remarkable energy distribution of 25.6% and 74.4% for the wind turbine system and the PV field, respectively. Additionally, the HRES implementation in Dakhla was projected to save a significant 128.21 tons of CO_2 emissions. In a related study by Adefarati and Bansal (2017), the integration of PV, wind turbines, diesel generators, and battery storage into power system generation was investigated. This approach not only reduced power interruptions but also lowered operational costs. To bolster electricity generation from PV, wind, and battery storage sources, a diesel generator model was incorporated into the distribution system. This integration concept not only enhanced distribution system reliability but also improved overall power system performance and efficiency.

On a different study, Thirunavukkarasu and Sawle (2021) tackled the optimal configuration of HRESs for sustainable and cost-effective load demand fulfilment. Using HOMER simulations, they delved into the techno-economics of standalone hybrid photovoltaic-wind turbine-diesel-battery-converter energy systems in Tamil Nadu, India. A multitude of system combinations was scrutinized based on technical parameters, costs, electrical power production from each source, and unmet load considerations. The outcomes of this study showcased that the off-grid solar-wind-diesel-battery configuration emerged as the most economical option across all sites, outperforming other system configurations. Remarkably, Thoothukudi city displayed the lowest cost of electricity (0.266 $/kWh) and net present cost of electricity (NPC) at 138,197 $. This was particularly economical when compared to a standalone diesel system, which resulted in a higher cost of electricity ($1.88) and an NPC of $977,523. Additionally, the standalone diesel operation produced 41,854 kg of CO_2 emissions, surpassing those associated with other renewable energy systems. On the other hand, Redouane et al. (2018) in their study of the technical and economic feasibility of implementing a hybrid energy system with storage for the fishing village of Lamhiriz along the southern coast of Morocco, selected as a pilot site. The proposed system integrates diesel and wind power, as well as electrochemical and thermal storage components. The study used two main approaches: an economic simulation using HOMER software and an optimization problem solved using the General Algebraic Modelling System (GAMS). Despite differences in the estimates of electrical installations between the two methods, the overall disparity in costs over a 20-year period for the village of Lamhiriz was found to be insignificant. The HOMER software facilitated detailed power generation and cost simulations, streamlining the process compared to optimization algorithms. Conversely, the optimization approach provided a more direct route to sizing and managing the system, with the financial analysis carried out separately. The study

concluded that renewable energy, in particular wind power, offers a competitive solution for powering isolated fishing villages, with hybrid systems proving viable even with minimal use of conventional back-up systems. The energy costs of the optimized hybrid system are juxtaposed with those of a conventional diesel system. The study showed that the energy cost of the optimal hybrid system is around 0.11 euros/kWh, which is much lower than the conventional system, which costs 0.297 euros/kWh. This study highlights the potential benefits of hybrid energy solutions for isolated fishing villages facing problems of energy access and cost.

In the case of our study, the objective is to examine the viability of a hybrid wind-photovoltaic energy system in the city of Dakhla, Morocco, focusing on its techno-economic feasibility for the provision of cost-effective clean energy. In contrast to the existing literature, our research uses GIS and virtual reality techniques to model the system, using the technical specifications of the site and the technical characteristics of its components to optimize its productivity. Furthermore, by evaluating its economic viability, our results suggest the possibility of attracting investors in the field of renewable energies to promote the development of this region of Morocco, which despite its potential, still relies heavily on non-renewable energy sources.

METHODOLOGY

The main objective of the methodology used is the installation of a hybrid photovoltaic-wind system with an installed power of 20 MW, harnessing high potential in the city of Dakhla. Connected to the local network, the system aims to reinforce the growing demand for electricity and ensure its continuity. The suitable site for the installation of the project was meticulously selected based on GIS coupled with Multi-Criteria Decision Analysis (MCDA) using Fuzzy Analytical Hierarchy Process (Fuzzy AHP) in a previous study we conducted at of the same study area (Achbab et al., 2020) as illustrated in Figure 1. This selection effectively integrates a series of climatic, economic, environmental and social factors that require accurate assessment. The optimal site was established through an exhaustive review of the availability of wind and solar resources, minimal shading and easy access to power and road networks. At the same time, comprehensive environmental and social impact assessments were carried out diligently. Then, taking into account the technical specifications of the system's components, which are mainly photovoltaic modules, inverters and wind turbines that exist on the market and have proved their worth in similar large-scale projects, the sizing of the system was established. The hybrid system will then be designed using modelling techniques in a computer-aided 3D virtual environment. The use of a virtual environment allows natural interaction between man and the 3D environment. The design of the hybrid system was guided by standards and constraints specific to the chosen site, aimed at optimizing its productivity. These considerations included the specifications of the mounting system, spacing between module rows, inclination, orientation, surface area, and topography of the site. This 3D model was enhanced with an orthophoto, georeferenced with exact geographic coordinates, ensuring precise alignment with the actual site context. Once the comprehensive 3D model was finalized, it was converted into a Digital Elevation Model (DEM) raster map format, presented with fine resolution (0.1 m) as illustrated in Figure 2. This facilitated more accurate quantification of solar radiation using algorithms integrated into ArcGIS software. The methodology adopted to assess the wind potential is based on the use of the Weibull distribution to statistically model wind speed data collected at the Dakhla meteorological station over a period of one year (2021) at hourly intervals. This approach offers numerous advantages for wind farms: it accurately adapts to real data, ensuring statistical reliability and robustness, enables comprehensive analysis over an extended timeframe, facilitates precise modelling of wind resources for optimized park design, enhances understanding of local wind regimes to support optimal planning of wind installations, and reduces financial risks by providing an accurate assessment of wind potential. Through the application of specific algorithms, a thorough evaluation of the system's annual and monthly productivity is conducted. The economic analysis of the system delves into the financial intricacies surrounding the integration, operation, and maintenance of this renewable energy solution. This comprehensive study encompasses various facets, beginning with a meticulous assessment of initial capital expenditures, spanning the costs of acquiring and installing essential components such as photovoltaic panels, wind turbines, inverters, and balance of the system. It extends further

to encompass ongoing operational and maintenance expenses, including monitoring, repairs, and potential replacements. Crucially, the economic viability of the hybrid system is scrutinized through a lens of financial feasibility, meticulously comparing total costs against potential revenue streams. This evaluation often involves complex metrics such as payback period, return on investment (ROI), NPV, and IRR, all aimed at determining the project's profitability and attractiveness. Moreover, the study explores revenue generation avenues by selling electricity. Sensitivity analysis identifies critical variables influencing financial outcomes. Ultimately, the economic study serves as a compass, guiding stakeholders in navigating the financial landscape of renewable energy investment, offering insights vital for informed decision-making and sustainable energy transition strategies. On the other hand, the environmental impact assessment within the study encompasses a multifaceted approach, considering various factors pivotal to understanding the sustainability implications of the hybrid system. Firstly, it delves into the life cycle greenhouse gas emissions associated with both wind and solar photovoltaic energy, meticulously scrutinizing the emissions stemming from each stage of their life cycle, from manufacturing to decommissioning. Additionally, the study conducts a greenhouse gas intensity assessment, providing insights into the emissions generated per unit of energy produced by wind and solar photovoltaic systems. Crucially, it estimates the greenhouse gas emissions avoided by the hybrid system, highlighting the significant contribution it makes to mitigating emissions compared to conventional energy sources.

TECHNICAL STUDY

Site selection

The process of selecting the optimal site for installing a wind-photovoltaic hybrid system involves an in-depth analysis of various criteria and constraints to improve performance and reduce costs. This study builds on previous research utilizing GIS and MCDA techniques, particularly the fuzzy analytical hierarchy process, to assess the potential of such a system in the city of Dakhla. Climatic, economic, and social factors were considered to identify suitable installation areas (Karipoğlu and Efe, 2023). This aspect of the study was previously conducted in the study area and was the subject of our publication (Achbab et al., 2020). Utilizing a four-class rating scale and exclusion zones, the study mapped the hybrid potential, thereby facilitating the selection of the most suitable location based on predefined criteria, as illustrated in Figure 1. This systematic

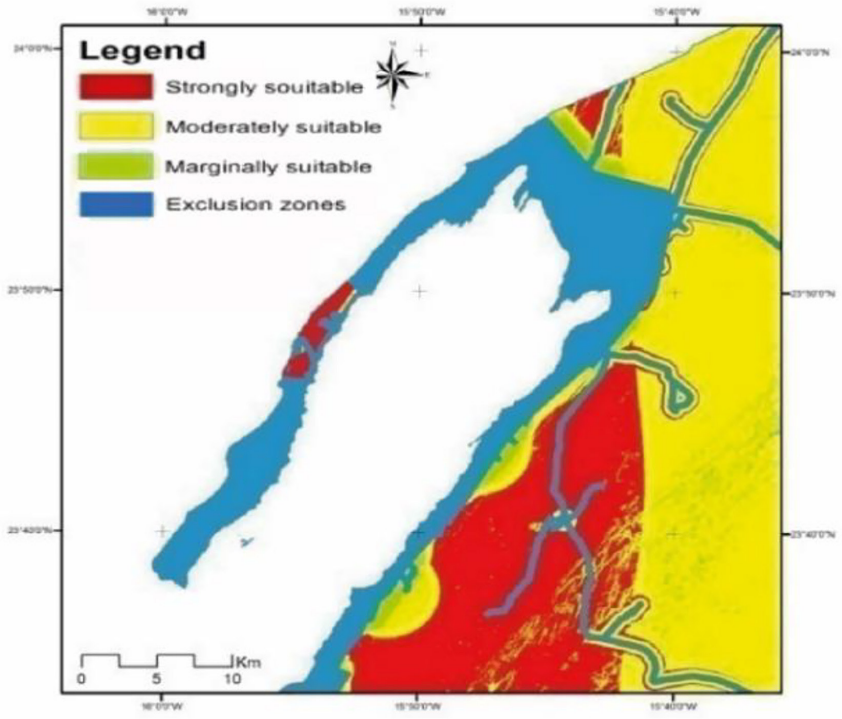

Figure 1. Map representing the wind-photovoltaic hybrid potential (Achbab et al., 2020)

approach ensures informed decision-making for identifying the site with the highest potential.

Sizing of the hybrid wind solar PV system

Ensuring the functionality, reliability, and longevity of a wind-solar PV hybrid system requires careful selection of components. This study prioritizes high-efficiency PV modules such as Trina Solar's TALLMAX TSM-PE14A, chosen for their ability to endure environmental conditions while maintaining consistent performance. Moreover, the selection of KACO New Energy's central inverters underscores the significance of reliability and efficiency in large-scale solar setups as shown in the study conducted by Roca Rubí (2018). These inverters, renowned for their advanced technology and dependable performance, are instrumental in converting direct energy from PV modules into usable alternating current for distribution. Concerning the wind energy, the adoption of Enercon's E82 turbine underscores reliability and power considerations, given Enercon's prominent stature in the industry. Table 1 gives an overview of the main components of the system

The sizing process is carried out taking into account the number of components, their type (in terms of technical characteristics, such as rated power, operating voltage range, etc.), and their arrangement in the installation field. The formulas used to size the solar PV plant are based on the article published by Kerekes et al. (2012). These results were then verified by using the System Advisor Model (SAM) software. SAM is a freely available desktop application designed to perform techno-economic analyzes of various energy technologies. It provides a valuable tool for project managers, engineers, policy analysts, technology developers and researchers, facilitating investigations into the technical, economic and financial viability of renewable energy projects. On the other hand, determining the appropriate number of WTs in a hybrid solar photovoltaic WT system involves a comprehensive assessment of energy demand, site characteristics, and renewable energy potential. By analyzing the energy requirements and available resources at the installation site, including wind patterns, and available land area, it becomes possible to select the optimal capacity for both WTs and solar photovoltaic panels. The goal is to achieve a balanced generation of energy from both wind and solar sources to meet overall energy demand while minimizing intermittency and variability. By having a study carried out on the site's wind power, we would be able to determine the power of a WT in real and local conditions before buying it. In this study, five WTs, model (E82) manufactured by Enercon with an average power of 2 MW was selected to assess the wind potential of the wind farm. The results of the calculations relating to the sizing are illustrated in Table 2.

The 3D modeling of the hybrid wind solar plant

Based on the sizing results obtained previously, this section focuses on the implementation of the hybrid system design using computer-assisted virtual reality (VR) technology. This makes it possible to create 3D simulation environments using software such as AutoCAD, Google SketchUp and ArcGIS, allowing natural interaction between users and the environment (Li et al., 2018). The hybrid system design follows site-specific standards and constraints to optimize productivity, including site topography, PV module area, row spacing, orientation and tilt angles. The analysis included the import and modification of the SketchUp file in Collada (.dae) format, to allow its analysis using GIS tools including ArcGIS software (Chow et al., A., 2014). this will allow its conversion into a DEM with a fine resolution (0.1 m) for precise quantification of solar radiation and shading. the integration of orthorectified aerial images and its georeferencing to precise geographic coordinates adds a realistic aspect to the model. The design of the photovoltaic solar power plant is shown in Figure 2.

Table 1. Main components of the hybrid system

PV technology		Wind turbine technology	
PV panels manufacturer	Trina solar	Wind turbine manufacturer	ENERCON GmbH
Model	TALLMAX TSM-PE14A	Model	E-82
Inverter manufacturer	KACO new energy	Rotor shaft height	80 m
Inverter model	Blue planet 2200 TL3	Number of wind turbines turbine	5
Installed power	10.18 MW	Installed power	10 MW
Solar power plant area	21 ha	Wind park area	33.6 ha

Table 2. Results of the various sizing parameters for the hybrid system

Solar PV energy		Wind turbine energy	
Number of panels in series (NS)	18	Rotor diameter	82 m
Number of parallel panels (NP)	442	Rotor shaft height	80 m
Numbers of inverters (VI)	4	Number of wind turbines turbine	5
Numbers of photovoltaic modules	31824	Installed power (MW)	10 MW
Power installed	10.18 MW	Number of rows	2
Total panels area S=NS*NP*VI*Spannel	6.19 ha	Separation distance	410m
Solar power plant area	21 ha	Area	33.6 ha

Resource assessment

Modeling solar irradiation and simulating photovoltaic energy generation

The efficiency of solar panels largely depends on the solar radiation they receive during their installation. Calculating overall solar radiation for each row of solar panels involves adding direct and diffuse solar radiation, a process facilitated by an algorithm built into ArGIS software. This calculation uses the DEM as input data, as described by Fu and Rich in 2002 and according to the following Equations.

$$Global_{tot} = Dir_{tot} + Dif_{tot} \quad (1)$$

$$Dir_{tot} = \Sigma Dir_{\theta,\alpha} \quad (2)$$

$$Dif_{tot} = \Sigma Dif_{\theta,\alpha}(11) \quad (3)$$

$$Dir_{\theta,\alpha} = SConst \cdot \beta m(\theta) \cdot SunDur_{\theta,\alpha} \cdot \cdot \mathrm{SunGap}_{\theta,\alpha} \cdot \cos(AngIn_{\theta,\alpha}) \quad (4)$$

$$Dif_{\theta,\alpha} = R_{glb} \cdot Pdif \cdot Dur \cdot \cdot SkyGap\theta,\alpha \cdot Weight_{\theta,\alpha} \cdot cos(AngIn_{\theta,\alpha}) \quad (5)$$

where: $Global_{tot}$ – the global solar radiation, Dir_{tot} – direct solar radiation, Dif_{tot} – diffuse solar radiation; *SConst* – the solar flux outside the atmosphere at the mean earth sun distance, known as solar constant. The value 1367 W/m^2 was used for the solar constant which is consistent with the World Radiation Center (WRC) solar constant; β – the transmissivity of the atmosphere (averaged over all wavelengths) for the shortest path (in the direction of the zenith); $m(\theta)$ – the relative optical path length, measured as a proportion relative to the zenith path length; $SunDur_{\theta,\alpha}$ – the time duration represented by the sky sector. For most sectors, it is equal to the day interval (for example, a month) multiplied by the hour interval (for example, a half hour). For partial sectors (near the horizon), the duration is calculated using spherical geometry; $SunGap_{\theta,\alpha}$ – the gap fraction for the *Sun* map sector; $AngIn_{\theta,\alpha}$ – the angle of incidence between the centroid of the sky sector and the axis normal to the surface; *Rglb* – the global normal radiation; *Pdif* – the proportion of global normal radiation flux that is diffused. Typically, it is approximately 0.2 for very clear sky conditions and 0.7 for very cloudy sky conditions; *Dur* – the time interval for analysis; $SkyGap_{\theta,\alpha}$ – the gap fraction (proportion of visible sky) for the sky sector; $Weight_{\theta,\alpha}$ – the proportion of diffuse.

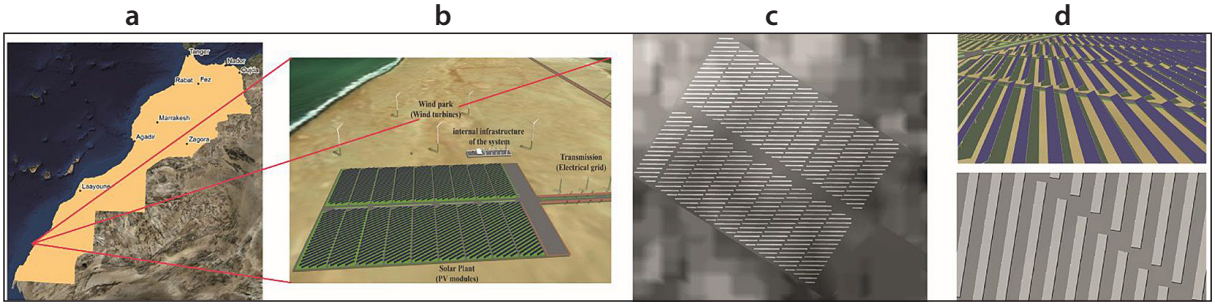

Figure 2. Hybrid system modeling: (a) site location, (b) 3D virtual modeling, (c) digital elevation model, (d) shading modeling of the hybrid

Based on this Equations, solar radiation quantification was carried out using ArcGIS software, analyzing the position of the sun and various factors to determine solar radiation levels at specific locations. The DEM generated from the virtual model was used for this analysis (Santos et al., 2014; Moudrý et al., 2019; Saad et al., 2018; Nelson et al., 2020; Echlouchi et al., 2017). The defined parameters include:

- latitude – automatically calculated (23°83') for determining declination and solar position; solar radiation calculation period – variable, ranging from daily to yearly,
- topographic parameters – slope and orientation derived from the area's DEM,
- diffuse radiation proportion – dependent on atmospheric conditions, typically around 0.3 for clear skies,
- transmittance – reflects the energy received in the atmosphere versus that reaching the earth's surface. Default value is 0.5 for clear skies, with a range from 0 to 1 (indicating no transmission to complete transmission, respectively).

The spatial analysis made it possible to generate annual and monthly solar maps or other time intervals as illustrated in Figure 3, providing detailed information on the solar irradiation coming from the photovoltaic modules. Using mask extraction and zonal statistics, monthly and annual average values of solar irradiation were extracted for each month of the year, see Figure 4. The results indicated significant solar resources at the site, with 3,958 hours of sunshine per year and an average annual global direct irradiation of approximately 2,402 kWh/m²/year, demonstrating substantial potential for energy production solar. To compute the monthly and yearly energy output for each row of photovoltaic panels and consequently for the entire solar power plant, we employed an algorithm integrated into ArcGIS software based on the formula developed by Wiginton et al., (2010):

$$E = GI \times e \times S \times Cl \tag{6}$$

where: E – annual energy production (kWh), GI – average global solar irradiance (kWh/m²),

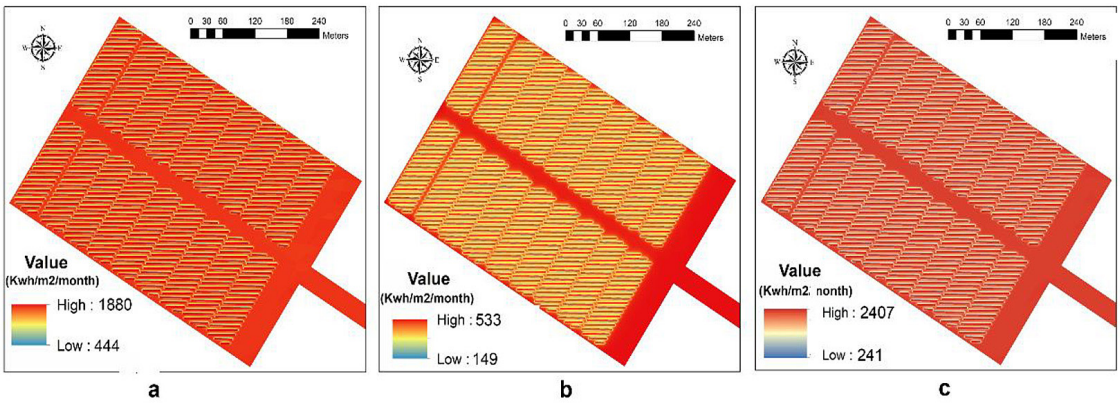

Figure 3. Modeling of solar irradiation in these three essential forms: a-direct, b-diffuse, c-global

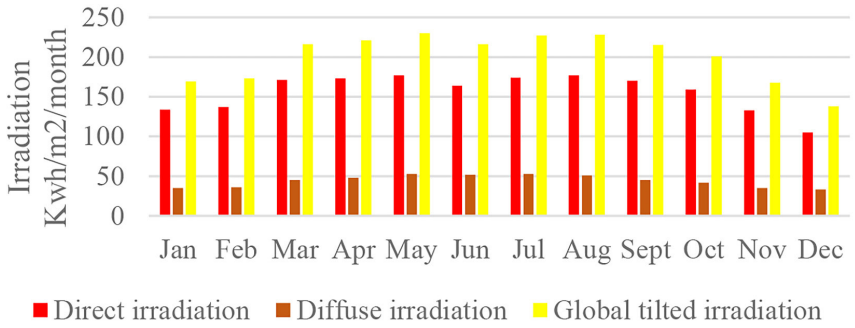

Figure 4. Variation of monthly solar irradiation at the level of PV solar panels in these three essential forms: direct, diffuse and global tilted irradiation

e – photovoltaic module efficiency (16.5%), *S* – surface area of solar panels, and *Cl* – loss coefficient or performance ratio (0.8).

The calculations reveal that the annual energy output of the 10 MW solar power plant amounts to approximately 19.63 GWh. This data is presented in Table 3, depicting the monthly productivity distribution of the central facility.

Mathematical modeling of wind speed and simulation of wind energy

To mathematically model wind speed, we use weather data from the city of Dakhla weather station for the year 2021 and at hourly intervals. The Weibull distribution, on the other hand, is a crucial tool for assessing the potential of wind energy and describing its probability distribution of wind speeds at a given location, as suggested by existing literature (Chaurasiya et al., 2018; George., 2014; Rocha et al., 2012; Saleh et al., 2012; Chang, 2011; De Andrade et al., 2014). This distribution is characterized by two parameters: the dimensionless shape parameter (*k*) and the scale parameter (*c*), which is measured in wind speed units (m/s). It is defined by its probability density function, denoted as *f*(*v*), and its cumulative distribution function, denoted as *F*(*v*). These functions are expressed through the following Equations (Deep et al., 2020; Bilir et al. 2015):

$$f(V) = \frac{K}{C}\left(\frac{V}{C}\right)^{K-1} e^{\left[-\left(\frac{V}{C}\right)^{K}\right]} \quad (7)$$

$$F(V) = 1 - e^{\left[-\left(\frac{V}{C}\right)^{K}\right]} \quad (8)$$

where: *v* – the wind speed. The distribution is called Rayleigh distribution when its shape parameter *k* is 2.

Several methods are used to determine the Weibull parameters. Among the most used are the graphical least squares adjustment method which is expressed as a logarithmic transformation of Equation 8 which could be expressed as Equation 9. In this method, the cumulative distribution function is transformed into a linear function Jamdade and Jamdade, (2012).

$$ln\,[-ln\,(1-F(V))] = K \times ln(V) - K \times ln(C) \quad (9)$$

$$Let\ xi = ln(Vi) \quad (10)$$

$$Yi = ln\,[ln\,(1 / [1 - F(Vi)])] \quad (11)$$

where: $i = 1, 2, 3, \ldots\ldots, n$.

The linear approximation of these data is obtained using the method of least squares, in the form

$$Y = a \times X + b \quad (12)$$

Thus, Weibull parameters are obtained as: $K = a$ and the scale parameter is:

$$C = e\text{^}((-b)/(k)) \quad (13)$$

On the other hand, the wind speed varies in an increasing way according to the height in the atmospheric boundary layers. Following this change in speed due to altitude, the wind speed measurements must be extrapolated to obtain those that correspond to the height of the hub of the wind turbine. By using the following relationship given in the study conducted by (Ouahabi et al., 2020), wind speeds at different heights obey a power law according to the following Equation 14:

$$Vh = Va \times (h/\mathrm{ha})\alpha \quad (14)$$

The exponent α is a constant that is influenced by the roughness of the topographic surface in the specific location. When wind speed is measured by an anemometer placed at a certain height (ha), the Weibull probability density function, characterized by the identified parameters Ka and Ca, can be employed to estimate wind speed values at various heights. The parameters of the Weibull distribution function, denoted as *Kh* and *Ch*, for an altitude (*h*) above the anemometer's level, are derived using the following relationships, as provided in (Ouahabi et al., 2020; tar et al., 2008; Abdelrahman et al., 2022; Khalfa et al., 2018).

$$Kh = Ka \times \left(\frac{1 - 0.088\,ln\left(\frac{ha}{10}\right)}{1 - 0.088\,ln\left(\frac{h}{10}\right)}\right) \quad (15)$$

$$Ch = Ca \times \left(\frac{h}{ha}\right)^{n} \quad (16)$$

$$\alpha = \left(\frac{X - 0.088ln(Ca)}{1 - 0.088ln\left(\frac{ha}{10}\right)}\right) \quad (17)$$

where: $X = 0.25$ for $0 <$ roughness ≤ 0.005 m; $X = 0.31$ for $0.005 \leqq$ roughness < 0.05 m; $X = 0.37$ for $0.05 \leqq < 0.5$ m; $X = 0.48$ for for $0.5 \leqq$ roughness < 4 m.

Based on the classification of roughness and the associated lengths for various typical landscapes provided by Khalfa et al. (2018), the roughness length at the site measures approximately 0.0024 meters. Once the parameters "*k*" and "*c*" of the Weibull distribution have been

determined, it becomes possible to visualize the fitted Weibull density curve on the wind speed histogram at different heights. Figure 5, illustrates the fit of the Weibull density function to the wind speed distribution observed for the different months of the year at a height of 10 meters. Once the parameters "*k*" and "*c*" of the Weibull distribution have been determined, it becomes possible to visualize the fitted Weibull density curve on the wind speed histogram at different heights. Figure 5, illustrates the fit of the Weibull density function to the wind speed distribution observed for the different months of the year 2021 at a height of 10 meters. To calculate the wind energy produced by a wind farm, routines are used that combine the power curve of the wind turbine given by the constrictor and the distribution of wind speeds observed on the site. The power curve converts the wind distribution into potential energy produced by the wind turbine. Suppose that wind speed measurements are available at regular intervals of width dV over a period of plus or minus one year, "*T*". The interval between each measurement is "dt" and the number of samples is "N" measurements. The duration of the observation period, "*T*", is therefore equal to $N \times$ dt. A sample of different speeds is obtained, from V1 up to VN. It is therefore possible to calculate the energy efficiency (*E*) during the period "*T*" by multiplying the power curve of the wind turbine (P) with intervals of frequency distribution of wind speed $f(V)$ calculated according to the Equation 18 recommended by Sliz-Szkliniarz and Vogt (2011).

$$E = T \times \sum_{k=1}^{N} Pk(Vk) \times f(Vk) \qquad (18)$$

In the context of wind energy production, it's crucial to consider various factors that can lead to reductions in output power from wind turbines. These factors include the wake effect caused by neighboring turbines, power interruptions due to grid capacity limitations, maintenance and environmental shutdowns, and environmental conditions such as dirt or ice accumulation on

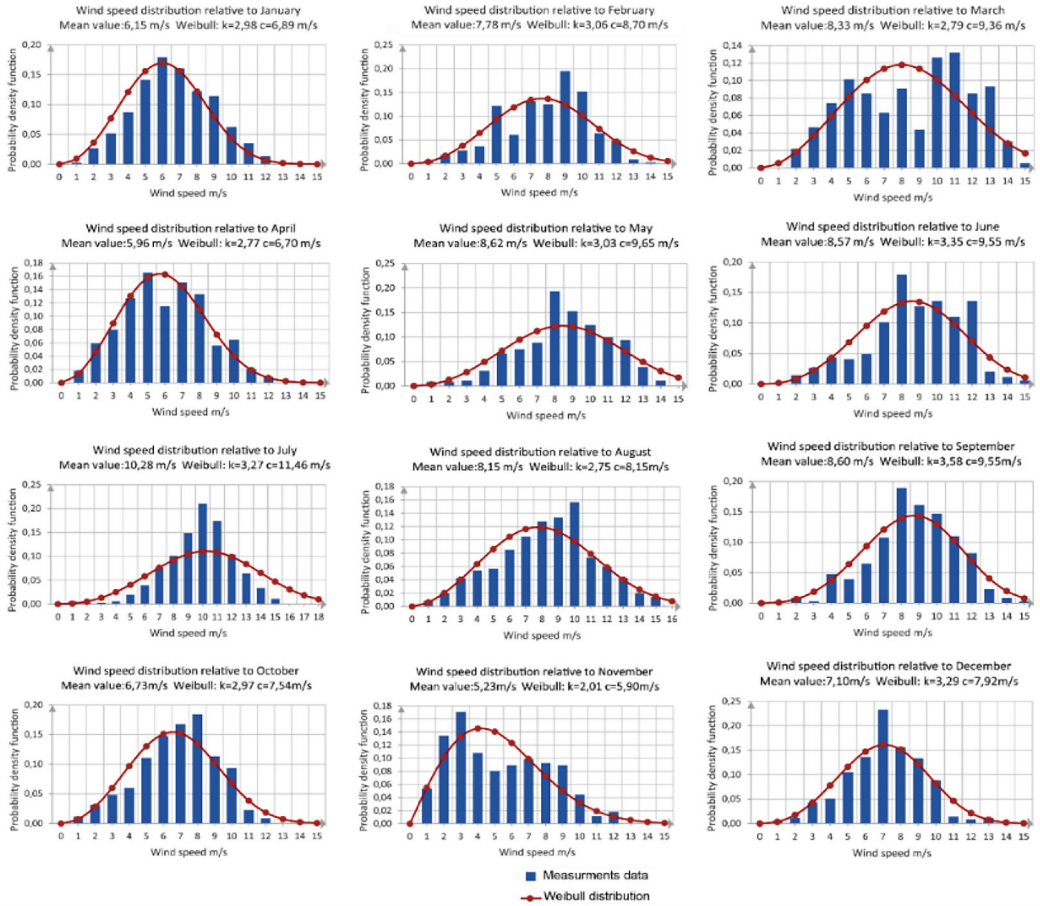

Figure 5. Weibull distribution of wind speed at the Dakhla meteorological station for the different months of the year 2021

turbine blades. Since specific data for individual turbines are often unavailable, an average loss factor is applied across all turbines. Following the approach used by Lehneis and Thrän (2023), a loss factor of approximately 16% was adopted in this study to ensure realistic simulation results for energy productivity. The monthly net energy produced by the wind farm, factoring in these losses, is detailed in Table 3.

Configuring and simulating the performance of hybrid systems

A hybrid wind-solar photovoltaic system provides adaptability to varying requirements, site conditions, and energy demands by leveraging the complementary nature of wind and solar resources. Its ability to ensure consistent power supply, even when one source is not operating optimally, enhances reliability compared to standalone systems. The system typically includes an AC bus for wind turbines and a DC bus for solar panels, with inverters converting solar-generated DC power to AC. Energy is fed to the grid through a common connection point (CPC) see Figure 6. Specific components and configuration may vary based on factors like wind farm size and location. Monthly energy productivity data reveals that the hybrid system generates approximately 60 GWh annually, with wind and solar power complementing each other and reaching peak production during summer months. This consistent energy availability improves system efficiency, reduces the need for energy storage and helps to reduce the economic cost of the project.

The simulated power production of the hybrid system is derived from the cumulative simulations of solar PV and wind substations. These individual simulations, previously obtained and carefully analyzed, constitute the basis for forecasting the combined energy production of the hybrid system. This approach ensures a more accurate representation of system performance, facilitating informed decision-making and effective system deployment planning. Table 3 and Figure 7 illustrates the monthly energy productivity of the hybrid system (MWh) and the contribution of solar PV and wind substations for the year 2021.

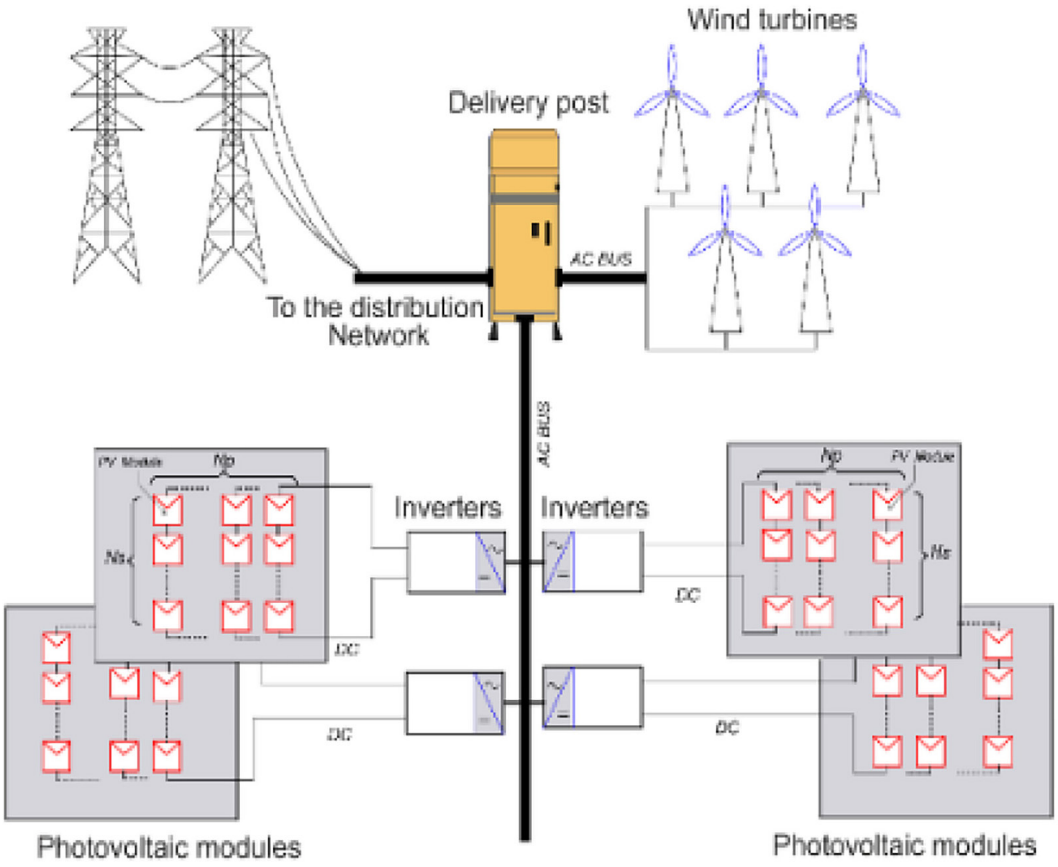

Figure 6. Block diagram of the wind-solar photovoltaic hybrid system

Table 3. Monthly energy productivity of the hybrid system in (MWh) during the year 2021

Month	Solar PV energy in MWh	Wind turbine energy in MWh	Hybrid wind-Pv energy in MWh
Jan	1381	2374	3755
Feb	1415	3259	4674
Mar	1765	3893	5658
Apr	1805	2176	3981
May	1873	4121	5994
June	1764	4032	5796
July	1852	4952	6804
Aug	1862	3782	5644
Sep	1755	4093	5848
Oct	1643	2835	4478
Nov	1377	1732	3109
Dec	1133	3130	4263
Total (MWh)	19,625.00	40,380.00	60,005.00

Results and discussion of technical analysis

The results of the technical study show that at the level of the solar power plant the average annual radiation is approximately 2402 kWh/m²/year, while the average annual wind power density at the height of the hub (80 meters) is approximately 433 W/m². Simulation of the system's productivity shows that the solar photovoltaic plant, with an installed capacity of 10.18 MW, can generate annual energy production of around 19,625 MWh, corresponding to a capacity factor of 22%. At the same time, the wind farm, with an installed capacity of 10 MW, supplies around 40,380 MWh of local energy per year, with a capacity factor of 46%. As a result, the hybrid wind-solar photovoltaic system, with a total capacity of 20.18 MW, achieves an annual energy production of 60 GWh, depending on local climatic conditions and component performance. This analysis highlights the complementary nature of these resources, ensuring both the availability and reliability of energy production while maintaining a high level of environmental efficiency.

ECONOMIC ANALYSIS

The levelized cost of electricity

The LCOE (levelized cost of electricity) is an important metric for assessing the economic viability of a large-scale wind-solar photovoltaic hybrid system. LCOE represents the average cost of producing one unit of electricity over the entire lifespan of the system. It is computed by dividing the total lifetime costs of the system by the total lifetime electricity production (Edalati et al., 2013).

To derive the LCOE, a meticulous approach is essential. This involves estimating both the capital costs of the system and its expected operating and maintenance expenses throughout its service life. The anticipated annual electricity production is determined, taking into account the system's capacity factor, which gauges actual output relative to maximum potential output over a specified period. However, LCOE calculations involve several assumptions and estimates and may not capture the full scope of economic benefits. The formula for LCOE, as outlined by (Edalati et al., 2013; Allouhi et al., 2019), is:

$$\mathrm{LCOE} = \frac{c_{I_0} + \sum_{t=1}^{L} \frac{Mt}{(1+r)^t}}{\sum_{t=1}^{L} \frac{Et}{(1+r)^t}} \qquad \text{With: } E_t = S_t(1 - d)^t \quad (19)$$

where: Et – the energy produced during year t; St – the annual energy output during the first-year operation; c_{I0} – initial investment cost of the HRES (USD) or the total capital expenditure (CAPEX); Mt – is the annual maintenance cost of the RES (USD); L – the lifetime of the system (years) where it is assumed that all the components will have the same life time (25 years); d – the degradation rate (%) of the PV systems over the specified period; r – the annual discount rate; d – the degradation rate (%) of the PV systems over the specified period.

In project evaluations, the choice of discount rate (r) significantly impacts the financial analysis,

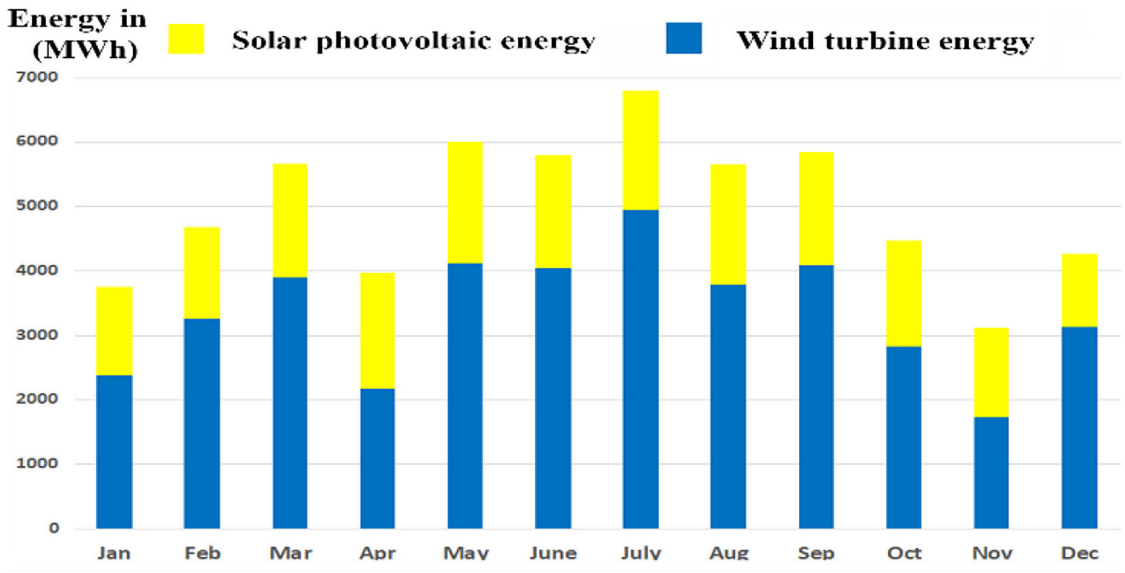

Figure 7. Contribution of solar and wind energy sources at the hybrid system in (MWh) during the year 2021

with different rates for public and private sector projects. Typically, public sector projects operate with a lower '*r*' of around 4–5% (Department of Public Expenditure, 2016), often regulated by law. In contrast, private sector projects tend to employ higher *r* values, ranging from 8–10%. The disparity primarily arises from the private sector's necessity to remunerate shareholders and achieve shorter-term returns (Ghazi et al., 2021). Capital costs (c_{I0}) are expressed in $/kW and are recorded at the project's delivery date. This temporal distinction has a substantial impact on cost due to discounting principles. Capital invested ten years before project initiation has a more pronounced effect on delivery cost due to time-related discounting, relative to capital invested at the project's outset.

Concerning the reliability and degradation of photovoltaic (PV) modules over their 25–30 – year lifespan, degradation can result from various factors such as packaging materials, semiconductor wear, and interconnection issues (Rajput et al., 2017). Recent studies suggest that a significant portion (78%) of PV panels degrade less than 1% annually, attributed to advancements in c-Si cells, with an average degradation rate of 0.8–0.9% per year (Edalati et al., 2013). For our analysis, an assumed average degradation rate of 0.85% is utilized for photovoltaic modules.

As for wind turbines, studies show they experience an average annual power loss of 1.6 ± 0.2%, with load factors decreasing from 28.5% when new to 21% at the age of 19 years. This consistent trend applies to various turbine generations and wind farms. This degradation results in a 12% reduction in wind farm output over a twenty-year lifetime, subsequently elevating the LCOE by 9%. However, the rate of degradation is subject to variations influenced by factors like component quality, maintenance practices, and operating conditions. Regular maintenance and inspections play a pivotal role in identifying and addressing issues before they escalate. Our analysis assumes an average degradation rate of 0.64% for wind turbines, as per the study conducted by (Mathew et al., 2022).

Calculation of the initial investment cost or the capital expenditure of the HRES

In the economic evaluation of a large-scale wind-solar photovoltaic system, the initial investment cost plays an important role. It encompasses the one-time expenses associated with the system's installation, making it a critical factor in assessing project financial viability. To conduct a comprehensive financial analysis, it is essential to account for all project-related expenses, including these initial capital costs. The initial capital cost estimation for this project involves considering various components, such as PV modules, wind turbines, inverters, step-up transformers, system balance components (BOS), civil works, and land (Tran and Smith., 2018). The formula employed to calculate the initial investment cost is as follows:

$$I_{invest\ Cost} = C_{Wind} \times C_{WT} + C_{Solar} \times C_{Panel} + C_{Inverter} + \\ + C_{BOS} + C_{GridConnection} + C_{Land} + C_{Rep} + C_{Other} \quad (20)$$

where: C_{Wind} represents the installed capacity of the wind turbines (in kW); C_{WT} represents the cost per unit capacity of wind turbines (in \$/kW); C_{Solar} represents the installed capacity of the solar PV panels (in kWp); C_{Panel} represents the cost per unit capacity of solar PV panels (in \$/kWp); $C_{Inverter}$ represents the cost of the inverters (in \$); C_{BOS} represents the cost of components and equipment necessary for the functioning and integration of the renewable energy system, albeit not directly involved in the energy conversion process; $C_{GridConnection}$ represents the cost of grid connection infrastructure (in \$); C_{Land} represents the cost of land; C_{Rep} represents the cost of replacing components over the project's 25 – year lifespan; C_{Other} encompasses any additional costs associated with balance of system components, civil works, land acquisition, permits, and other relevant expenditures (in \$).

Calculation of the operations and maintenance cost of the HRES plant

Operations and maintenance (O&M) are essential for ensuring an HRES operates at peak efficiency throughout its lifespan. O&M activities encompass a range of tasks, including routine inspections and maintenance of components such as solar panels, inverters, and batteries (if applicable) (Mohammadi et al., 2016; Fazelpour et al., 2017; Minaeian et al., 2017). It also involves the upkeep of equipment like blades, gearbox, and other parts, monitoring and analyzing system performance to identify and address issues. O&M also involves ensuring compliance with safety and environmental regulations as well as training and managing staff responsible for plant operation and maintenance (Minaeian et al., 2017). The expected maintenance requirements and associated costs can be estimated based on the manufacturer's recommendations and industry standards (Mohammadi et al., 2016; Fazelpour et al., 2017; Minaeian et al., 2017). Additionally, the operational history of similar solar PV plants can provide valuable insight into the expected O&M costs.

Furthermore, a relationship exists between the O&M cost per unit of capacity and the total O&M cost for a HRES. The O&M cost per unit of capacity represents expenses attributed to each installed capacity unit (usually expressed in \$/MW/year) (Tran and Smith., 2018). The relationship is expressed as:

$$Total_{O\&M\ \mathrm{Cost}} = O\&M\ cost\ per\ unit\ capacity \times \\ \times\ Total\ installed\ capacity \quad (21)$$

where: $Total_{O\&M\ cost}$ – the annual O&M cost for the entire hybrid system (in \$/year); *O&M cost per unit capacity* – the O&M cost per MW of installed capacity (in \$/MW/year); *total installed capacity* – the combined installed capacity of wind turbines and solar PV panels in the hybrid system (in MW).

This relationship allows for estimating total O&M expenses based on the O&M cost per unit of capacity and the hybrid system's size. Note that the O&M cost per unit of capacity can vary based on technology, location, maintenance needs, and industry standards, necessitating accurate values tailored to specific project characteristics (Tran and Smith., 2018).

Financial analysis

Any investor in a renewable energy project is faced with multiple risks, which may be linked to the intermittency of the resource, regulatory uncertainties or public acceptance. Investment choices, whose financial dimension will contribute to increasing or sometimes reducing the value of the project, must therefore be made with full knowledge of the risks involved. Valuation is a crucial stage in the decision-making process for investment projects. It gives investors the means to thoroughly assess the economic and financial feasibility of their projects. This assessment is based on key criteria, including NPV, IRR, discounted payback period (DPP) and return on investment (ROI). These tools, widely used in various industries, are rooted in the discounted cash flow method. This method uses a discounting technique to take account of the time value of money, allowing anticipated future values to be converted into their present-day equivalents.

$$Present\ value = \frac{Future\ value}{(1+Discount\ rate)} \times 100 \quad (22)$$

Net present value

The net present value (NPV) is a crucial financial tool in the renewable energy sector, extensively used for evaluating the economic feasibility

and potential profitability of renewable energy projects and for making comparisons between investment options (Abdelhady, 2021). NPV calculations help determine whether an investment in a renewable energy project is financially viable, indicating positive or negative returns. A positive NPV suggests that the project is expected to generate more cash inflows than outflows, indicating financial viability, while a negative NPV implies a lack of financial profitability. The NPV is computed by discounting future cash flows using a specified discount rate, with a higher NPV indicating greater financial attractiveness (Abdelhady, 2021). The formula for NPV is as follows:

$$NPV = \left[\sum_{t=1}^{L} \frac{CF_t}{(1+r)^t} \right] - I_0 \quad (23)$$

where: CF_t – the net cash flows in the year t and (CF – total net cash flow); r – the discount rate; I_0 – the initial investment.

Internal rate of return

The internal rate of return (IRR) is an important financial metric used to assess the profitability and appeal of an investment or project. It signifies the average annual rate of return expected from an investment throughout its anticipated lifespan. This percentage represents the discount rate at which the present value of cash inflows matches that of cash outflows. IRR is a percentage Figure used to gauge potential returns against a desired rate of return or benchmark, aiding in the assessment of an investment's feasibility and financial viability. IRR is a valuable tool in investment decision-making, facilitating comparisons between investment options. Higher IRRs are typically preferred by investors as they promise greater returns. When evaluating multiple projects, the one with the highest IRR is generally favoured, assuming all other factors are equal.

$$\left[\sum_{t=1}^{L} \frac{CF_t}{(1+r)^t} \right] - I_0 = 0 \quad (24)$$

Discounted payback period

The "payback period" in renewable energy projects represents the adjusted time it takes for the project to recover its initial investment through generated revenues or savings (Edalati et al., 2013; Nazir et al., 2020). It signifies when the project reaches the break-even point and begins generating positive cash flows. This metric is crucial for assessing the financial feasibility and profitability of renewable energy projects. The revised recovery period can be affected by various factors, including changes in project parameters, such as design modifications, equipment cost reductions, fluctuations in electricity prices, and adjustments in financing arrangements. These updates can impact financial projections and the time needed for the project to recoup its initial investment. To calculate the payback period, one seeks to find the smallest duration (tpb) for which:

$$\left[\sum_{t=1}^{tpb} \frac{CF_t}{(1+r)^t} \right] \geq I_0 \quad (25)$$

where: I_0 – the initial investment costs with the project.

Return on investment

Return on investment (ROI) stands for return on investment. It is a financial metric used to measure the profitability and efficiency of an investment. ROI represents the percentage of the return or profit gained in relation to the initial investment amount. To calculate ROI, the net profit or gain from the investment is divided by the initial investment cost, and the result is multiplied by 100 to express it as a percentage. The formula for ROI is as follows:

$$ROI = \frac{Net\ profit}{Initial\ investment} \times 100 \quad (26)$$

A higher ROI signifies a more profitable investment, indicating that the returns surpass the initial investment substantially.

ENVIRONMENT ANALYSIS

Life cycle greenhouse gas emission from wind and solar PV energy

In a general context, lifecycle analysis involves scrutinizing a specific aspect, termed the functional unit, of an entity, process, or product throughout its entire lifespan (Allouhi et al., 2019). In this investigation, the emphasis is placed on both wind and solar photovoltaic electricity generators, with the functional unit being the greenhouse gas (GHG) intensity measured in grams of CO_2 - equivalent emissions per kilowatt-hour (CO_2 eq/kWh) of electricity produced. Evaluating the emissions associated with PV and wind entails considering several lifecycle stages. Existing literature highlights four pivotal stages: material sourcing

and manufacturing, installation, operation and maintenance, and decommissioning. This section delves into a comprehensive analysis of each of these stages.

Assessing the greenhouse gas intensity of wind and solar PV energy

In the evaluation of the GHG emissions throughout the lifecycle of wind and solar PV energy, Nugent and Sovacool (2014) emphasise that while these energy sources are generally considered low-carbon, they are not entirely devoid of carbon emissions. Wind power exhibits an emissions intensity ranging from 0.4 g CO_2 - eq/kWh to 364.8 g CO_2 - eq/kWh, with an average of 34.11 g CO_2-eq/kWh. Similarly, solar energy shows variability from 1 g CO_2 - eq/kWh to 218 g CO_2 - eq/kWh, with an average of 49.91 g CO_2 - eq/kWh. These findings underscore the significance of acknowledging the presence of carbon emissions associated with these energy sources, albeit at relatively lower levels.

Estimating avoided GHG emissions by the hybrid system

In evaluating the potential reduction of GHG emissions achieved by the hybrid system, this section primarily focuses on carbon dioxide (CO_2), a significant contributor to global warming. The study specifically targets the reduction of CO_2 emissions facilitated by the hybrid system. To quantify the environmental benefits, the avoided CO_2 emissions linked to solar PV systems are calculated based on the assumption that each kilowatt-hour of electricity generated by the hybrid system displaces an equivalent amount of electricity produced by conventional energy systems. The avoided CO_2 emissions in tones is represented by the Equation 27 (Allouhi et al., 2016).

$$AE = \frac{Ec \times Fcm}{1000} \tag{27}$$

where: *EC* denotes the energy generated by the hybrid wind-solar PV system (measured in kWh) during a specified reference period, and *Fcm* represents the carbon mitigation factor. The emission factor for the Moroccan electricity mix is estimated to be 746 g CO_2/kWh.

ECONOMIC AND FINANCIAL DATA

Estimated total investment cost for the hybrid wind-solar PV system

The estimation of the total investment cost for a 20.18 MW wind-photovoltaic hybrid system involves a thorough analysis of both wind and solar components, taking into account various factors such as equipment expenses, engineering costs, licensing fees, and other technology-specific expenditures (Tran and Smith, 2018). To gather cost-related information, a range of reliable sources, including the U.S. Energy Information Administration (EIA), the National Renewable Energy Laboratory (NREL) cost database, and relevant literature, including research by (Tran and Smith, 2018; De Arce et al., 2012), were consulted. This analysis encompasses various crucial cost components, such as wind turbine CAPEX, rotor, nacelle, tower, BOS CAPEX (Balance of System Capital Expenditure), engineering costs, project management expenses, foundation expenditures, site access and facilities costs, assembly and installation outlays, electrical infrastructure expenses, financial CAPEX, construction financing, and contingency expenses (Tran and Smith, 2018).

The cost evaluation of implementing the hybrid system also benefits from prior research on individual wind and PV systems, as well as insights from Barker et al., (2021), who provided valuable cost data and a modeling tool to assess the installation cost of hybrid wind-photovoltaic systems. Table 4 and Figure 8 depict the average breakdown of investment costs by hybrid system power generators CAPEX, BOS CAPEX, and O&M CAPEX.

RESULTS AND DISCUSSION ON ECONOMIC AND ENVIRONMENTAL ASPECTS

Life cycle energy analysis of the hybrid wind-solar PV system

The proposed hybrid system generates an annual electricity output of 60,005.00 MWh, as shown in Table 3. This energy output corresponds to a capacity factor (CF) of 34%. We have based our analysis on the previous results on the evolution of the energy productivity of its subsystems over their lifetime described above. The calculations indicate a rate of energy degradation of the hybrid system estimated at around 9% over its

lifetime of 25 years. Figure 9, provides a visual representation of the annual energy production's evolution over the projected lifespan, outlining the expected changes in energy generation throughout the years.

The levelized cost of electricity relating to the hybrid system

By inputting the relevant parameters such as the discount rate (6%), the projected lifespan of the wind turbines, installation costs, and operating and maintenance expenses, we obtained an levelized cost of electricity (LCOE) value of 0.045/kWh. Significantly, this LCOE value is lower than the current electricity price in Morocco, which stands at $0.0830/kWh. This outcome holds immense advantages for both investors and the government, underscoring the feasibility and viability of this technology.

Cash flow analysis and environmental impact of the hybrid wind-solar PV system

Similarly, the economic viability of the hybrid system cash flow analysis is assessed through key financial metrics, including the NPV, IRR, and payback period. The income generated by the hybrid system is calculated by multiplying its annual energy production (AEP) by the selling price of electricity. To account for the time value of money, the NPV of the hybrid system is determined using a discount rate of 6%. The analysis results indicate an NPV of $27,439,559, an IRR of 17.5%, an estimated payback period of 8 years, representing the time needed to recover the initial investment cost, and a net profit at the end of lifetime of USD 89,769,689.00. In addition, and from an environmental point of view, the hybrid system can avoid a quantity of GHG of the order of 936,494 tones CO_2eq over its lifecycle, which means a saving in CO_2 of the order of USD 18,729,875.00. Table 5,

Table 4. Investment and O&M costs of hybrid wind-solar PV technology ($/kW) according to various sources

Hybrid wind-solar PV technology	
Parameter	Value
Wind turbine CAPEX	1,029.00($/kW)
Photovoltaic module CAPEX	470.00$/KW
Foundation	55($/kW)
Site preparation	29($/kW)
Substation	28($/kW)
Grid connection	17($/kW)
Collection	58($/kW)
Erection	19($/kW)
Management and development	129($/kW)
Module racking	103($/kW)
BOS CAPEX	438.00($/kW)
O&M cost	25.65($/Kw-year)
Life time	25 years
Hybrid wind-solar PV system power installed	20.18 MW
Wind turbine substation power installed	10 MW
Solar PV substation power installed	10.18 MW
Total investment cost	1,826.26.00($/kW)

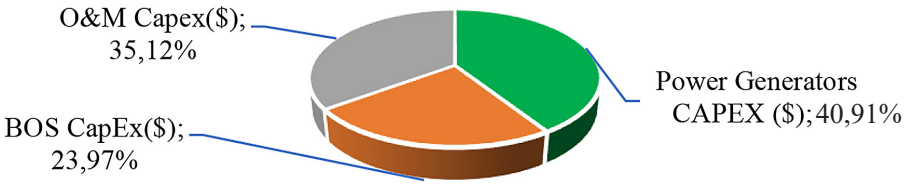

Figure 8. Breakdown of CAPEX by item of expenditure for the HRES in percentages

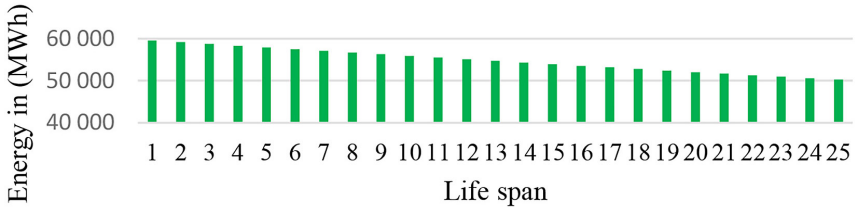

Figure 9. Evolution the energy produced by the hybrid system over 25 years

provides a detailed overview of these financial and environmental parameters and Figure 10 shows the discounted and undiscounted cash flows for the hybrid wind-solar PV system. As illustrated in Figure 10, the impact of discounting can be seen graphically. The discounted payback period is estimated at 8 years, compared with 7 years for the undiscounted pay back period.

Sensitivity analysis

Sensitivity analysis is an essential process in economic modeling, assessing the robustness of models by varying key variables within specified ranges. It's commonly used in evaluating investment projects to account for uncertainties in costs, income, and investment value. By identifying risks and uncertainties, sensitivity analysis aids in making informed investment decisions and understanding which variables are most sensitive to risk. It helps in managing sector risks effectively by determining break-even points and developing support proposals. Key reasons for utilizing sensitivity analysis include accounting for measurement errors, imprecise factors, and understanding the impact of unpredictable events on project outcomes. In this project, sensitivity analysis involves varying five critical variables - initial investment cost, discount rate, energy produced, electricity purchase price, and O&M costs - by ±30% while keeping others constant, and the results are analyzed to gauge the sensitivity of NPV. The results obtained from this analysis are presented in Tables 6. The sensitivity analysis reveals the varying degrees of influence different variables have on the NPV as illustrated in Table 6. Among them, the energy produced and the electricity selling price exhibit a substantial impact on NPV sensitivity. When both values increase by 30%, the NPV jumps by over 165% (from $27,439,559.00 to $45,241,208), and when they decrease by 30%, the NPV drops by 65% (from $27,439,559.00 to $9,637,910.00). The discount rate also affects NPV sensitivity, albeit to a lesser extent. A 30% increase in the discount rate results in a 27% decrease in NPV (from $27,439,559.00 to $20,089,879.00), while a 30% decrease leads to a 135% increase (from

Table 5. Summary of the financial and environmental results of implementing the hybrid system

Hybrid wind-solar photovoltaic	
Project lifetime (year)	25
Power installed (MW)	20.18
Capacity factor (CF)	34%
Specific yield (kWh/kWp)	2,973.00
Initial investment cost (USD)	23,905,440.00
Life span energy production, MWh	1,369,580.00
Cost of energy used ($/ kWh)	0,083
Discount rate	6%
Net present value (NPV) in (USD)	27,439,559.00
Internal rate of return (IRR)	17.5%
Net profit at the end of lifetime (USD)	89,769,689.00
Payback period	8 years
Return of investment	222 %
LCOE($/kwh)	0.045
Avoided GHG emissions (CO_2) during lifetime	936,494.00 tones CO_2eq
GHG emissions pricing (Gain in CO_2) during lifetime (USD)	18,729,875.00

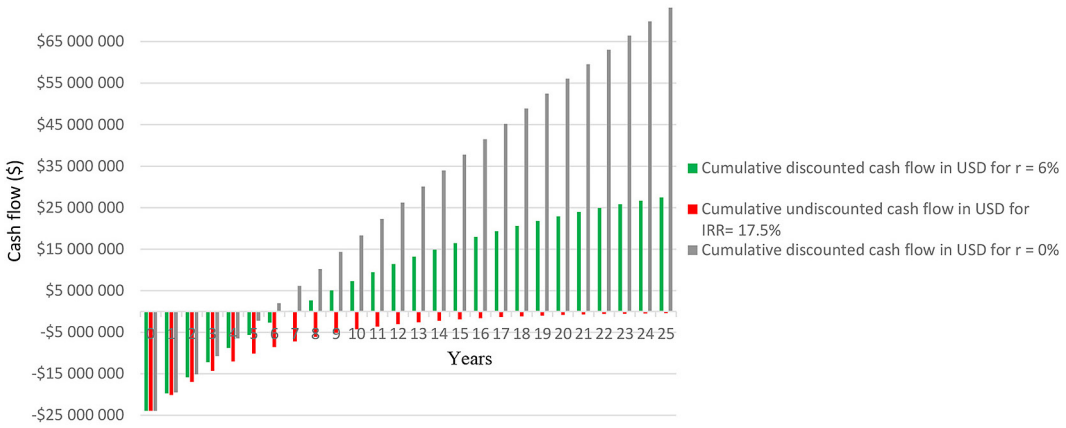

Figure 10. Cumulative cash flows analysis of the hybrid system project using different discount rates

Table 6. Sensitivity analysis of the NPV

Specification	-30%	-20%	-10%	0%	10%	20%	30%
Energy produced	9,637,910	15,571,793	21,505,676	27,439,559	33,373,442	39,307,325	45,241,208
Electricity selling price	9,637,910	15,571,793	21,505,676	27,439,559	33,373,442	39,307,325	45,241,208
Discount rate	36,963,627	33,501,435	30,337,073	27,439,559	24,781,531	22,338,784	20,089,879
Initial investment cost	34,611,191	32,220,647	29,830,103	27,439,559	25,049,015	22,658,471	20,267,927
O&M	29,837,709	29,038,325	28,238,942	27,439,559	26,640,176	25,840,793	25,041,410

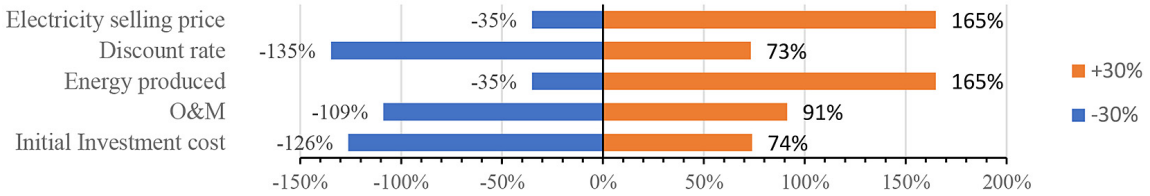

Figure 11. Sensitivity analysis of NPV for various key parameters

$27,439,559.00 to $36,963,627.00). Next in line is the cost of the initial investment in the hybrid system. When increased by 30%, the NPV falls by 26% (from $27,439,559.00 to $20,267,927.00), and when decreased by 30%, the NPV rises by 126% (from $27,439,559.00 to $346,111,191.00). Lastly, the cost of operating and maintaining the hybrid system impacts the NPV. A 30% increase in this cost results in a 9% NPV decrease (from $27,439,559.00 to $25,041,410.00), while a 30% decrease leads to a 109% NPV increase (from $27,439,559.00 to $29,837,709.00). While the energy produced and electricity selling price have the most significant effects on NPV, it is essential to consider all variables as they contribute significantly to the project's financial outlook. The tornado diagram of NPV sensitivity provides an overview, as shown in Figure 11.

CONCLUSIONS

Thanks to our rigorous and comprehensive technical, economic and environmental analysis, we have been able to quantitatively assess the long-term viability and profitability of the hybrid wind-photovoltaic system. By Taking into account modeling that integrates GIS and virtual reality (VR) for precise and immersive analysis of energy productivity, system investment costs, operating and maintenance expenses, potential revenue streams and projected savings over time, we can provide a sound economic model for the implementation of this sustainable energy solution. Through meticulous simulations, crucial economic variables such as LCOE, IRR, NPV and ROI have been identified as key considerations for local energy project developers. Our results will provide a basis for informed decision-making and demonstrate the viability of the system to stakeholders. Furthermore, it is crucial to emphasize the importance of determining avoided GHG emissions (CO_2) and GHG emissions pricing (Gain in CO_2). These factors play a significant role in assessing the environmental impact and economic feasibility of renewable energy projects. By accurately quantifying the reduction in greenhouse gas emissions achieved through the implementation of the hybrid wind-photovoltaic system and assigning appropriate monetary value to these emissions reductions, we can better understand the full extent of the project's environmental benefits and its contribution to mitigating climate change and improved air quality and public health.

It should also be noted that beyond the commendable reductions in carbon emissions and the mitigation of climate change, this transition will create significant economic opportunities. It will stimulate local job creation, reduce dependence on imported fossil energy sources, and promote technological advances in the renewable energy sector. By seizing the opportunities offered locally through investment in renewable energies, Dakhla can serve as a model for other regions, demonstrating that it is possible to achieve a harmonious balance between economic prosperity and environmental well-being.

Acknowledgment

The authors wish to express their gratitude and thanks to the entire academic staff of the Geosciences Laboratory of the Ain Chock Faculty of Sciences, for their availability and in particular their judicious advice which contributed to the writing of this article and provided us with the methodological tools essential to its conduct. Finally, the authors thank all the reviewers for taking the time to review our manuscript.

REFERENCES

1. Abdelhady, S. 2021. Performance and cost evaluation of solar dish power plant: sensitivity analysis of levelized cost of electricity (LCOE) and net present value (NPV). Renewable Energy, 168, 332–342.
2. Abdelrahman, M.A., Abdel-Hamid, R.H., Abo Adma, M.A., Daowd, M. 2022. Techno-economic analysis to develop the first wind farm in the Egyptian western desert at Elkharga Oasis. Clean Energy, 6(1), 211–225.
3. Achbab, E., Rhinane, H., Maanan, M., Saifaoui, D. 2020. Developing and applying a GIS-Fuzzy AHP assisted approach to locating a hybrid renewable energy system with high potential: Case of Dakhla region–Morocco. In 2020 IEEE International conference of Moroccan Geomatics (Morgeo), 1–6.
4. Adefarati, T., Bansal, R.C. 2017. Reliability assessment of distribution system with the integration of renewable distributed generation. Applied energy, 185, 158–171.
5. Allouhi, A., Saadani, R., Buker, M.S., Kousksou, T., Jamil, A., Rahmoune, M. 2019. Energetic, economic and environmental (3E) analyses and LCOE estimation of three technologies of PV grid-connected systems under different climates. Solar Energy, 178, 25–36.
6. Allouhi, A., Saadani, R., Kousksou, T., Saidur, R., Jamil, A., Rahmoune, M. 2016. Grid-connected PV systems installed on institutional buildings: Technology comparison, energy analysis and economic performance. Energy and Buildings, 130, 188–201.
7. Arslan, T., Bulut, Y.M., Yavuz, A.A. 2014. Comparative study of numerical methods for determining Weibull parameters for wind energy potential. Renewable and Sustainable Energy Reviews, 40, 820–825.
8. Barker, A., Bhaskar, P., Anderson, B., Eberle, A. 2021. Potential infrastructure cost savings at hybrid wind plus solar PV plants (No. NREL/TP-5000-78912). National Renewable Energy Lab.(NREL), Golden, CO (United States).
9. Bilir, L., İmir, M., Devrim, Y., Albostan, A. 2015. An investigation on wind energy potential and small scale wind turbine performance at İncek region–Ankara, Turkey. Energy Conversion and Management, 103, 910–923.
10. Chang, T.P. 2011. Performance comparison of six numerical methods in estimating Weibull parameters for wind energy application. Applied Energy, 88(1), 272–282.
11. Chaurasiya, P.K., Ahmed, S., Warudkar, V. 2018. Study of different parameters estimation methods of Weibull distribution to determine wind power density using ground based Doppler SODAR instrument. Alexandria Engineering Journal, 57(4), 2299–2311.
12. Chow, A., Fung, A.S., Li, S. 2014. GIS modeling of solar neighborhood potential at a fine spatiotemporal resolution. Buildings, 4(2), 195–206.
13. Dale, M. 2013. A comparative analysis of energy costs of photovoltaic, solar thermal, and wind electricity generation technologies. Applied sciences, 3(2), 325–337.
14. De Andrade, C.F., Neto, H.F. M., Rocha, P.A.C., da Silva, M.E.V. 2014. An efficiency comparison of numerical methods for determining Weibull parameters for wind energy applications: A new approach applied to the northeast region of Brazil. Energy conversion and Management, 86, 801–808.
15. De Arce, R., Mahía, R., Medina, E., Escribano, G. 2012. A simulation of the economic impact of renewable energy development in Morocco. Energy Policy, 46, 335–345.
16. Deep, S., Sarkar, A., Ghawat, M., Rajak, M.K. 2020. Estimation of the wind energy potential for coastal locations in India using the Weibull model. Renewable energy, 161, 319–339.
17. Department of Public Expenditure. 2016. The Public Spending Code: E – Technical References. http://www.per.gov.ie/en/project-discount-inflation-rates.
18. Echlouchi, K., Ouardouz, M., Bernoussi, A.S. 2017. Urban solar cadaster: application in North Morocco. In 2017 International Renewable and Sustainable Energy Conference (IRSEC),1–7.
19. Edalati, S., Ameri, M., Iranmanesh, M., Tarmahi, H., Gholampour, M. 2016. Technical and economic assessments of grid-connected photovoltaic power plants: Iran case study. Energy, 114, 923–934.
20. El-Houari, H., Allouhi, A., Salameh, T., Kousksou, T., Jamil, A., El Amrani, B. 2021. Energy, Economic, Environment (3E) analysis of WT-PV-Battery autonomous hybrid power plants in climatically varying regions. Sustainable Energy Technologies and Assessments, 43, 100961.
21. Fazelpour, F., Markarian, E., Soltani, N. 2017. Wind energy potential and economic assessment of four locations in Sistan and Balouchestan province in Iran. Renewable Energy, 109, 646–667.
22. Fu, P., Rich, P.M. 2002. A geometric solar radiation model with applications in agriculture and

forestry. Computers and electronics in agriculture, 37(1–3), 25–35.

23. George, F. 2014. A comparison of shape and scale estimators of the two-parameter Weibull distribution. Journal of Modern Applied Statistical Methods, 13(1), 3.
24. Ghazi, F.E., Sedra, M.B., Akdi, M. 2021. Energy transition from fossil to renewable sources in North Africa: Focus on the renewable electricity generation in Morocco. International Journal of Energy Economics and Policy, 11(3), 236–242.
25. Jamdade, P.G., Jamdade, S.G. 2012. Analysis of wind speed data for four locations in Ireland based on Weibull distribution's linear regression model. International Journal of Renewable Energy Research, 2(3), 451–455.
26. Karipoğlu, F., Ozturk, S., Efe, B. 2023. A GIS-based FAHP and FEDAS analysis framework for suitable site selection of a hybrid offshore wind and solar power plant. Energy for Sustainable Development, 77, 101349.
27. Kerekes, T., Koutroulis, E., Séra, D., Teodorescu, R., Katsanevakis, M. 2012. An optimization method for designing large PV plants. IEEE Journal of Photovoltaics, 3(2), 814–822.
28. Khalfa, D., Benretem, A., Cheikchouk, N., Herous, L. 2018. Comparative study of wind speed extrapolation methods for sites with different roughness. International Journal of Power and Energy Conversion, 9(3), 205–227.
29. Elamouri M., Ben Amar F. 2008. Wind energy potential in Tunisia. Renew Energy, 33, 758–68.
30. Lehneis, R., Thrän, D. 2023. Temporally and Spatially Resolved Simulation of the Wind Power Generation in Germany. Energies, 16(7), 3239.
31. Li, Z., Cheng, Y., Yuan, Y. 2018. Research on the application of virtual reality technology in landscape design teaching. Educational Sciences: Theory & Practice, 18(5).
32. Mathew, M.S., Kandukuri, S.T., Omlin, C.W.P. 2022. Estimation of wind turbine performance degradation with deep neural networks.
33. Minaeian, A., Sedaghat, A., Mostafaeipour, A., Akbar, A.A. 2017. Exploring economy of small communities and households by investing on harnessing wind energy in the province of Sistan-Baluchestan in Iran. Renewable and Sustainable Energy Reviews, 74, 835–847.
34. Mohammadi, K., Mostafaeipour, A., Sedaghat, A., Shamshirband, S.,Petković, D. 2016. Application and economic viability of wind turbine installation in Lutak, Iran. Environmental Earth Sciences, 75(3), 1–16.
35. Moudrý, V., Beková, A., Lagner, O. 2019. Evaluation of a high resolution UAV imagery model for rooftop solar irradiation estimates. Remote Sensing Letters, 10(11), 1077–1085.
36. Nazir, M.S., Wang, Y., Bilal, M., Sohail, H.M., Kadhem, A.A., Nazir, H.R., Ma, Y. 2020. Comparison of small-scale wind energy conversion systems: economic indexes. Clean Technologies, 2(2), 144–155.
37. Nelson, J.R., Grubesic, T.H. 2020. The use of LiDAR versus unmanned aerial systems (UAS) to assess rooftop solar energy potential. Sustainable Cities and Society, 61, 102353.
38. Nugent, D., Sovacool, B.K. 2014. Assessing the lifecycle greenhouse gas emissions from solar PV and wind energy: A critical meta-survey. Energy Policy, 65, 229–244.
39. Ouahabi, M.H., Elkhachine, H., Benabdelouahab, F., Khamlichi, A. 2020. Comparative study of five different methods of adjustment by the Weibull model to determine the most accurate method of analyzing annual variations of wind energy in Tetouan-Morocco. Procedia Manufacturing, 46, 698–707.
40. Ouali, H.A.L., Raillani, B., El Hassani, S., Moussaoui, M.A., Mezrhab, A., Amraqui, S. 2020. Techno-economic evaluation of very large-scale photovoltaic power plant, case study: Eastern Morocco. In 2020 5th International Conference on Renewable Energies for Developing Countries (REDEC), 1–5.
41. Rajput, P., Tiwari, G.N., Sastry, O.S. 2017. Thermal modelling with experimental validation and economic analysis of mono crystalline silicon photovoltaic module on the basis of degradation study. Energy, 120, 731–739.
42. Redouane, A., Acouetey, P., El Hasnaoui, A., El Harraki, I. 2018. Feasibility Study of Energy Hybrid Systems for Villages of the Southern Moroccan Coastline. In: 2018 6th International Renewable and Sustainable Energy Conference (IRSEC), 1–6.
43. Roca Rubí, Á. 2018. Design and modelling of a large-scale PV plant. Master's thesis, Universitat Politècnica de Catalunya.
44. Rocha, P.A.C., de Sousa, R.C., de Andrade, C.F., da Silva, M.E.V. 2012. Comparison of seven numerical methods for determining Weibull parameters for wind energy generation in the northeast region of Brazil. Applied Energy, 89(1), 395–400.
45. Saad, N.M., Hamid, J.R.A., Saraf, N.M., Halim, M.A., Idris, A.N., Khalid, N. 2018. Insolation Model from LiDAR-Derived Topographical Surface Models. In 2018 IEEE 8th International Conference on System Engineering and Technology (ICSET), 133–138.
46. Saleh, H., Aly, A.A.E.A., Abdel-Hady, S. 2012. Assessment of different methods used to estimate Weibull distribution parameters for wind speed in Zafarana wind farm, Suez Gulf, Egypt. Energy, 44(1), 710–719.
47. Santos, T., Gomes, N., Freire, S., Brito, M.C., Santos, L., Tenedório, J.A. 2014. Applications of solar mapping in the urban environment. Applied

Geography, 51, 48–57.

48. Sliz-Szkliniarz, B., Vogt, J. 2011. GIS-based approach for the evaluation of wind energy potential: A case study for the Kujawsko–Pomorskie Voivodeship. Renewable and Sustainable Energy Reviews, 15(3), 1696–1707.
49. Tar, K. 2008. Some statistical characteristics of monthly average wind speed at various heights. Renewable and Sustainable Energy Reviews, 12(6), 1712–1724.
50. Thirunavukkarasu, M., Sawle, Y. 2021. A comparative study of the optimal sizing and management of off-grid solar/wind/diesel and battery energy systems for remote areas. Frontiers in Energy Research, 9, 752043.
51. Tran, T.T., Smith, A.D. 2018. Incorporating performance-based global sensitivity and uncertainty analysis into LCOE calculations for emerging renewable energy technologies. Applied energy, 216, 157–171.
52. Wiginton, L.K., Nguyen, H.T., Pearce, J.M. 2010. Quantifying rooftop solar photovoltaic potential for regional renewable energy policy. Computers, Environment and Urban Systems, 34(4), 345–357.